Title

The HIV-1 reservoir in eight patients on long-term suppressive antiretroviral therapy is stable with few genetic changes over time

Journal

Proceedings of the National Academy of Sciences of the United States of America, 110(51)

ISSN

0027-8424

Authors

Josefsson, Lina
von Stockenstrom, Susanne
Faria, Nuno R
et al.

Publication Date

2013-12-17

DOI

10.1073/pnas.1308313110

Peer reviewed

The HIV-1 reservoir in eight patients on long-term suppressive antiretroviral therapy is stable with few genetic changes over time

Lina Josefsson[a,b,1], Susanne von Stockenstrom[a,b], Nuno R. Faria[c], Elizabeth Sinclair[d], Peter Bacchetti[e], Maudi Killian[d], Lorrie Epling[d], Alice Tan[d], Terence Ho[d], Philippe Lemey[c], Wei Shao[f], Peter W. Hunt[d], Ma Somsouk[d], Will Wylie[g], Daniel C. Douek[g], Lisa Loeb[d], Jeff Custer[d], Rebecca Hoh[d], Lauren Poole[d], Steven G. Deeks[d], Frederick Hecht[d,2], and Sarah Palmer[a,b,h,i,2]

[a]Department of Diagnostics and Vaccinology, Swedish Institute for Infectious Disease Control, 171 82 Solna, Sweden; [b]Department of Microbiology, Tumor and Cell Biology, Karolinska Institutet, 171 82 Solna, Sweden; [c]Department of Microbiology and Immunology, Rega Institute, Katholieke Universiteit, 3000 Leuven, Belgium; [d]Department of Medicine, University of California, San Francisco, CA 94110; [e]Department of Epidemiology and Biostatistics, University of California, San Francisco, CA 94143; [f]Advanced Biomedical Computing Center, Science Applications International Corporation–Frederick, Inc., National Cancer Institute–Frederick, Frederick, MD 21702; [g]Human Immunology Section, Vaccine Research Center, National Institute of Allergy and Infectious Diseases, National Institutes of Health, Bethesda, MD 20892; and [h]Centre for Virus Research, Westmead Millennium Institute, Westmead, NSW 2145, Australia; and [i]Sydney Medical School, The University of Sydney, Sydney, NSW 2006, Australia

Edited by Robert F. Siliciano, The Johns Hopkins University School of Medicine, Baltimore, MD, and accepted by the Editorial Board October 17, 2013 (received for review May 6, 2013)

The source and dynamics of persistent HIV-1 during long-term combinational antiretroviral therapy (cART) are critical to understanding the barriers to curing HIV-1 infection. To address this issue, we isolated and genetically characterized HIV-1 DNA from naïve and memory T cells from peripheral blood and gut-associated lymphoid tissue (GALT) from eight patients after 4–12 y of suppressive cART. Our detailed analysis of these eight patients indicates that persistent HIV-1 in peripheral blood and GALT is found primarily in memory CD4$^+$ T cells [CD45RO$^+$/CD27($^{+/-}$)]. The HIV-1 infection frequency of CD4$^+$ T cells from peripheral blood and GALT was higher in patients who initiated treatment during chronic compared with acute/early infection, indicating that early initiation of therapy results in lower HIV-1 reservoir size in blood and gut. Phylogenetic analysis revealed an HIV-1 genetic change between RNA sequences isolated before initiation of cART and intracellular HIV-1 sequences from the T-cell subsets after 4–12 y of suppressive cART in four of the eight patients. However, evolutionary rate analyses estimated no greater than three nucleotide substitutions per gene region analyzed during all of the 4–12 y of suppressive therapy. We also identified a clearly replication-incompetent viral sequence in multiple memory T cells in one patient, strongly supporting asynchronous cell replication of a cell containing integrated HIV-1 DNA as the source. This study indicates that persistence of a remarkably stable population of infected memory cells will be the primary barrier to a cure, and, with little evidence of viral replication, this population could be maintained by homeostatic cell proliferation or other processes.

Combinational, antiretroviral therapy (cART) effectively suppresses but does not eradicate HIV-1 infection (1). Persistent low-level HIV-1 can still be detected in plasma (2–7) and cellular reservoirs (8–10) even after several years of suppressive cART, and cessation of current treatments invariably results in resumption of viral replication. Resting-memory CD4$^+$ T cells are a well-defined reservoir of HIV-1, and the reservoir is established when an activated CD4$^+$ T cell becomes infected by HIV-1 but transitions to a resting state (9) or perhaps when resting cells are infected directly (11–13). Central and transitional memory T cells have recently been identified as major contributors to the HIV-1 reservoir in the memory T-cell population (14). Naïve T cells have also been demonstrated to contain HIV-1 DNA in patients on suppressive therapy, although at a lower infection frequency than the memory T-cell population (15). In addition, many other cell types, including monocyte/macrophages, have been proposed to play a role in HIV-1 persistence (reviewed in ref. 16). These long-lived HIV-1–infected cells have been detected in peripheral blood. Several studies, however, suggest that the reservoir is largely established and maintained in lymphoid tissues, and that the infected cells circulating in blood may not be representative of the population of infected cells in tissue. For example, the majority of lymphocytes are sequestered in the gastrointestinal tract, and gut-associated lymphoid tissue (GALT) has been shown to be a major viral reservoir in patients on suppressive antiretroviral therapy (17–22).

In addition to the persistence of long-lived, latently infected cells, low-level viral replication has been proposed as a mechanism that maintains HIV-1 during cART. If complete viral replication cycles persist, despite suppressive antiretroviral therapy, this would lead to de novo cellular infection and a constant replenishment of the viral reservoir. Investigations into whether HIV-1 replication continues during suppressive therapy have been carried out with peripheral blood and GALT samples but have led to potentially contradictory results. Some studies have found an absence of genetic evolution in viral reservoirs (23–29) and no reduction of plasma RNA during intensification of cART

Significance

Identifying the source and dynamics of persistent HIV-1 during combinational antiretroviral therapy (cART) is crucial for understanding the barriers to curing HIV infection. Through genetic characterization of HIV-1 DNA in infected cells from peripheral blood and gut-associated lymphoid tissue from patients after long-term suppressive cART, our study reveals that the primary barrier to a cure is a remarkably stable pool of infected memory CD4$^+$ T cells. Through in-depth phylogenetic analyses, we determined that the HIV-1 reservoir in these cells from eight patients is kept stable during long-term cART and, with little evidence of viral replication, this population could be maintained by homeostatic cell proliferation or other processes.

Author contributions: L.J., F.H., and S.P. designed research; L.J., S.v.S., E.S., M.K., L.E., A.T., T.H., W.W., and S.P. performed research; P.W.H. and M.S. collected gut-associated lymphoid tissue samples; L.L., J.C., R.H., and L.P. recruited patients; E.S., L.E., P.L., W.S., P.W.H., M.S., and D.C.D. contributed new reagents/analytic tools; L.J., N.R.F., E.S., P.B., P.L., F.H., and S.P. analyzed data; and L.J., N.R.F., S.G.D., F.H., and S.P. wrote the paper.

The authors declare no conflict of interest.

This article is a PNAS Direct Submission. R.F.S. is a guest editor invited by the Editorial Board.

[1]To whom correspondence should be addressed. E-mail: Lina.Odevall@gmail.com.

[2]F.H. and S.P. contributed equally to this work.

This article contains supporting information online at www.pnas.org/lookup/suppl/doi:10.1073/pnas.1308313110/-/DCSupplemental.

(30, 31), suggesting that cART is effective in preventing viral replication in these anatomical sites. In contrast, increased numbers of 2-long terminal repeat circles in peripheral blood mononuclear cells and decreased amounts of unspliced HIV-1 RNA in $CD4^+$ T cells isolated from the terminal ileum have been reported during raltegravir intensification, supporting the concept that some viral replication can occur despite suppressive cART (32, 33). Thus, the role of on-going replenishment via cycles of replication as a cause of persistence is not fully understood.

To investigate the source and dynamics of HIV-1 reservoirs in peripheral blood and GALT, we sorted and genetically characterized intracellular HIV-1 from subsets of memory T cells, naïve T cells, and myeloid cells from these two compartments from eight patients who had been on suppressive therapy with undetectable viral loads (<40–75 copies/mL) for 4–12 y: five who initiated therapy during acute/early infection and three who initiated therapy during chronic infection. Our aim was to investigate the nature of the infected cell population during cART and explore the role of HIV-1 replication, as reflected by nucleotide sequence substitutions in maintaining this reservoir. Our study revealed that both memory T cells and naïve T cells harbor HIV-1 DNA after long-term suppressive therapy, and the infection frequency of these T cells was higher in patients treated during chronic infection compared with patients treated during early infection. In-depth phylogenetic analysis revealed little or no change in viral structure or divergence over time within the viral sequences isolated from the different T-cell populations compared with sequences isolated from plasma collected just before initiation of cART, indicating lack of on-going replication during long-term suppressive therapy.

Results

Higher Infection Frequency in Cells Isolated from Patients Treated During Chronic Infection Compared with Patients Treated During Acute/Early Infection. To assess the frequency of infected cells in peripheral blood and GALT in patients on suppressive therapy, we sorted different cell types from these compartments from eight patients on long-term suppressive antiretroviral therapy, five of whom initiated therapy during acute/early infection (1–3 mo of infection before initiation of therapy, patients 1–5) and three who initiated therapy during chronic infection (>1 y of infection before initiation of therapy, patients 6–8) (Table 1). We sorted central/transitional and effector memory T cells, naïve T cells, and myeloid cells from peripheral blood and GALT based on their specific cellular phenotypes (Fig. S1). We included more patients treated during acute/early infection (when their HIV-1 populations are homogeneous) as this allows us to genetically characterize HIV-1 populations after passing through different selective pressures related to cell type and tissue type. Due to the fact we are analyzing HIV-1 DNA extracted from infected cell lysates, we cannot distinguish whether the HIV-1 DNA under analysis is integrated, linear, or circular, and whether it will produce replication-competent virus. However, recent studies have shown that after 1 y of suppressive therapy, the majority of intracellular HIV DNA is integrated into the cellular genome and that total DNA and integrated DNA measurements are equivalent (34).

For each peripheral blood sample, specific $CD4^+$ T-cell subsets were sorted based on their cellular phenotypes until at least 200,000–1,000,000 cells of each T-cell subtype were collected. After these cells were sorted, the remaining memory T cells were sorted together (combining central/transitional and effector). We then conducted single–HIV-1 DNA sequencing on specific numbers of each cellular subset and estimated the HIV-1 infection frequency in each cell type using a maximum likelihood (ML) statistical analysis. When specific T-cell subsets were analyzed from peripheral blood, we found that the central/transitional memory and effector memory cells had a geometric mean HIV-1 infection frequency of 0.002% and 0.009%, respectively, in patients treated during acute/early infection (patients 1–5). The same two $CD4^+$ T-cell subsets had a geometric mean HIV-1 infection frequency of 0.04% and 0.02%, respectively, in those treated during chronic infection (patients 6–8) (Table 2, columns 1–4). The infection frequencies for peripheral blood central/transitional memory cells were 16-fold higher in the patients who were treated during chronic infection, whereas the infection frequency for peripheral blood effector memory cells was twofold higher in those treated during chronic versus acute/early infection (Table S1). HIV-1–infected peripheral blood naïve T cells were found in seven of the eight patients (patients 2–8) with a frequency of infection ranging from 0.0001% to 0.002% in patients 2–5 and from 0.002% to 0.04% in patients 6–8 (Table 2, columns 7 and 8). This equated to an 11-fold higher HIV-1 infection frequency of the naïve T cells isolated from the patients treated during chronic infection compared with patients treated during acute/early infection ($P = 0.05$, likelihood ratio test, Table S1). When combining all T cells from peripheral blood, we found a ninefold difference in infection frequency between patients treated during early versus chronic infection ($P = 0.023$, likelihood ratio test, Table S1). In addition, we determined the percentage of the total viral reservoir in peripheral blood T cells contributed by different T-cell subsets. As shown in Table 3, we found that the central/transitional memory T cells were the major component of the viral reservoir in all of the patients [mean percentage contribution = 56.3% (patients 2–8)], except for patients 6 and 7. In these two patients, the viral reservoir was found to persist predominantly in the naïve T cells

Table 1. Patient demographics

	Viral load; RNA copies per mL		CD4+ T-cell count; cells per μL					
Patient	Pretherapy	On-therapy[a]	Pretherapy	On-therapy	Length of infection, y	Time on therapy, y	Time of infection before initiation of therapy	Therapeutic regimen[b]
				Initiated therapy during early infection				
1	88,359	<40	165	470	8.6	8.5	1 mo	EFV/FTC/TDF
2	44,960	<40	494	1,048	7.9	7.6	2.5 mo	FPV, TDF/FTC, RTV
3	40,930	<40	792	1,279	12.8	12.5	3 mo	TDF/FTC, NVP
4	3,583	<40	648	867	6.7	6.6	1 mo	EFV/FTC/TDF
5	118,888	<40	243	571	4.3	4.2	1 mo	EFV/FTC/TDF
				Initiated therapy during chronic infection				
6	85,999	<40	406	491	7.3	5.3	2 y	EFV/FTC/TDF
7	74,117	<40	400	726	11.5	9	2.5 y	NVP, TDF/FTC
8	70,510	<40	342	891	10.6	8.8	1.8 y	EFV/FTC/TDF

[a]Viral RNA levels at the time of the study.
[b]Therapeutic regimen at time of sample isolation. To see all regimens used, see Table S3. EFV, efavirenz; FPV, fosamprenavir; FTC, tenofovir; NVP, nevirapine; RTV, ritonavir; TDF, emtricitabine.

Table 2. Frequency of infection: Peripheral blood

	1	2	3	4	5	6	7	8	9	10
	Central/transitional memory, CD45RO$^+$ CD27$^+$		Effector memory, CD45RO$^+$ CD27$^-$		All memory, CD45RO$^+$ CD27$^{-/+}$		Naïve, CD45RO$^-$ CD27$^+$		Myeloid, CD3$^-$ CD4$^+$	
Patient	Estimated frequency of infection, %	95% CI	Estimated frequency of infection, %	95% CI	Estimated frequency of infection, %	95% CI	Estimated frequency of infection, %[a]	95% CI	Estimated frequency of infection, %[a]	95% CI
					Initiated therapy during acute/early infection					
1	N/A	N/A	N/A	N/A	0.0076	0.0065, 0.0090	0	0.0000, 0.0006	0	0.0000, 0.0002
2	0.0229	0.0172, 0.0304	0.0089	0.0055, 0.0146	0.0156	0.0128, 0.0191	0.0022	0.0016, 0.0031	0, (0.00001)	0.0000, 0.0001 (0.000004, 0.00003)
3	0.0045	0.0032, 0.0064	0.0099	0.0072, 0.0137	0.0055	0.0040, 0.0075	0.0003	0.0002, 0.0005	0	0.000000, 0.0002
4	0.0004	0.0002, 0.0006	0.0010	0.0005, 0.0021	0.0006	0.0003, 0.0011	0.0001	0.0000, 0.0003	0	0.0000, 0.0002
5	0.0434	0.0308, 0.0611	0.0857	0.0667, 0.1099	0.1797	0.1420 0.2275	0.0023	0.0016, 0.0034	0, (0.00005)	0.0000, 0.0002 (0.000008, 0.0004)
					Geometric mean frequency of infection: Early infection					
1–5	0.0022	0.0000042, 0.019	0.0093	0.0003, 0.0490	0.0073	0.0003, 0.0360	0.0006	0.0005, 0.0008	0.00001	0.000004, 0.00002
					Initiated therapy during chronic infection					
6[b]	0.0333	0.0262, 0.0425	0.0025	0.0017, 0.0038	0.1252	0.0991, 0.1581	0.0374	0.0290, 0.0481	0, (0.0003)	0.0000, 0.0001 (0.0001, 0.0005)
7	0.0299	0.0225, 0.0398	0.2581	0.2099, 0.3172	0.1624	0.1340, 0.1968	0.0221	0.0167, 0.0292	0	0.0000, 0.0002
8	0.0460	0.0369, 0.0573	0.0826	0.0632, 0.1080	0.0296	0.0213, 0.0412	0.0022	0.0016, 0.0031	0	0.0000, 0.0003
					Geometric mean frequency of infection: Chronic infection					
6–8	0.0360	0.028, 0.047	0.0160	0.0000009, 0.2000	0.088	0.029, 0.20	0.007	0.0060, 0.0082	0.0001	0.00007, 0.0003

Numbers in parentheses denote the frequency of infection found in myeloid lysate with TCRs present. CI, confidence interval.

[a]One cannot rule out the possibility of low-but-nonzero infection rates in cases where estimates were zero, as shown by the upper confidence bounds.

[b]The low HIV-1 infection frequency of effector memory T cells and high HIV-1 infection frequency of naïve T cells from this patient was confirmed also 6 mo later.

Table 3. Percentage of the total viral reservoir in T cells contributed by different T-cell subsets

1	2	3	4	5	6	7
Patient	Overall percent infection[a]	Lower 95% CI	Upper 95% CI	Central/transitional memory; % contribution	Effector memory; % contribution	Naïve; % contribution
			Peripheral blood			
1				N/A		
2	0.0093	0.0071	0.0110	80.6	4.40	15.0
3	0.0030	0.0023	0.0036	53.2	41.5	5.30
4	0.0003	0.0002	0.0005	63.0	27.8	9.20
5	0.0420	0.0320	0.0520	62.3	36.5	1.20
6	0.0330	0.0270	0.0390	45.6	0.49	53.9
7	0.0640	0.0540	0.0740	14.1	67.5	18.4
8	0.0290	0.0240	0.0350	75.1	21.5	3.30
Mean percentage contribution				56.3	28.5	15.2
			GALT			
1				N/A		
2	0.0280	0.0150	0.0450	43.90	56.10	0.0
3	0.0190	0.0050	0.0350	55.20	44.80	0.0
4	0.0055	0.0000	0.0280	0.0	100.0	0.0
5	0.0079	0.0046	0.0110	18.20	71.20	10.60
6	0.1300	0.0980	0.1600	55.30	41.60	3.10
7	0.1100	0.0810	0.1400	4.80	93.50	1.70
8	0.0430	0.0300	0.0590	28.70	71.30	0.0
Mean percentage contribution				29.4	68.4	2.2

[a]Central/transitional and effector memory and naïve T cells combined.

(53.9%, patient 6) or effector memory T cells (67.6%, patient 7). The mean percentage for the effector memory T cells was 28.5% and for naïve T cells 15.2% (patients 2–6, Table 3).

We performed similar studies using GALT. We collected a total of 1,000–160,000 cells of the same $CD4^+$ T-cell populations in samples from GALT and found a geometric mean HIV-1 infection frequency of central/transitional memory T cells of 0.008% and 0.04% for patients treated in acute/early versus chronic infection, respectively. The geometric mean HIV-1 infection frequencies of effector memory T cells from GALT were 0.03% and 0.15% in patients treated during acute/early and chronic infection, respectively (Table 4, columns 1–4). This equated to a fivefold higher frequency of infection in the central/transitional memory populations and a sixfold higher frequency of infection

Table 4. Frequency of infection: GALT

	1	2	3	4	5	6	7	8
	Central/transitional memory, $CD45RO^+$ $CD27^+$		Effector memory, $CD45RO^+$ $CD27^-$		Naïve, $CD45RO^-$ $CD27^+$		Myeloid, $CD3^-$ $CD4^+$	
Patient	Estimated frequency of infection, %[a]	95% CI	Estimated frequency of infection, %	95% CI	Estimated frequency of infection, %[a]	95% CI	Estimated frequency of infection, %[a]	95% CI
				Initiated therapy during acute/early infection				
1	0.0280	0.0117, 0.0675	0.0269	0.0087, 0.0835	N/A	N/A	0	0.0000, 0.0169
2	0.0221	0.0115, 0.0425	0.0390	0.0210, 0.0724	0	0.0000, 0.1108	0	0.0000, 0.0640
3	0.0149	0.0056, 0.0396	0.0304	0.0098, 0.0942	0	0.0000, 0.3181	0	0.0000, 0.0273
4	0	0.0000, 0.0152	0.0132	0.0033, 0.0529	0	0.0000, 0.1209	0	0.0000, 0.0124
5	0.0019	0.0006, 0.0060	0.0228	0.0142, 0.0367	0.1365	0.0342, 0.5452	0, (0.0081)	0.0000, 0.012 (0.0020, 0.0324)
				Geometric mean frequency of infection: Early infection				
1–5	0.008	0.0051, 0.0120	0.026	0.018, 0.035	0.026	0.0044, 0.0810	0.0024	0.0004, 0.0075
				Initiated therapy during chronic infection				
6	0.1180	0.0848, 0.1641	0.1429	0.0960, 0.2128	0.6975	0.3497, 1.3915	0, (0.0297)	0.0000, 0.0084, (0.0169, 0.0523)
7	0.0106	0.0040, 0.0282	0.2152	0.1619, 0.2859	0.0962	0.0249, 0.3846	0, (0.0277)	0.0000, 0.0208, (0.0104, 0.0737)
8	0.0211	0.0123, 0.0364	0.1083	0.0750, 0.1563	0	0.000000, 0.018981	0, (0.0223)	0.0000, 0.0061, (0.0124, 0.0403)
				Geometric mean frequency of infection: Chronic infection				
6–8	0.04	0.0300, 0.0520	0.15	0.1300, 0.1900	0.052	0.0260, 0.0920	0.026	0.0170, 0.0370

Numbers in parentheses denote the frequency of infection found in myeloid lysate with TCRs present.
[a]One cannot rule out the possibility of low but nonzero infection rates in cases where estimates were zero, as shown by the upper confidence bounds.

in the effector memory T-cell population in the patients treated during chronic infection compared with patients treated during acute/early infection (Table S1). The difference between infection frequencies for these two patient groups was statistically significant for the effector memory population ($P < 0.0001$, likelihood ratio test) but showed only a trend toward a statistically significant difference for the central/transitional memory population ($P = 0.081$, likelihood ratio test). In one patient treated during acute/early infection and in all three patients treated during chronic infection, we isolated HIV-1–infected naïve T cells isolated from GALT. The infection frequency of naïve T cells from patients in which HIV-1 was detected in GALT ranged from 0.1% to 0.7% (Table 4, columns 5 and 6). In GALT, we also found a higher (fivefold) frequency of infection in the patients treated during chronic infection compared with the patients treated during acute/early infection, when all T cells from this compartment were combined ($P = 0.0004$, likelihood ratio test, Table S1). The mean percentage contribution of each cell type to the total viral reservoir in GALT was 29.4%, 68.4%, and 2.2% in central/transitional and effector memory and naïve T cells, respectively (Table 3, columns 5–7).

When comparing the HIV-1 infection frequency of T cells isolated from peripheral blood to GALT, we found a similar HIV-1 infection frequency of central/transitional and effector memory T cells from these two compartments. However, the infection frequency of naïve T cells from GALT was higher (nine times, all patients combined) compared with the infection frequency of these cells from peripheral blood ($P = 0.001$, likelihood ratio test, Table S1). When all T cells were combined, infection frequencies in T cells from GALT and peripheral blood were very similar.

As outlined above, when the contribution of each cell type to the overall reservoir was calculated, we found that most of the infection in blood was in central/transitional memory T cells (mean of 65% and 45% in patients treated during acute/early and chronic infection, respectively), whereas most of the infection in GALT was in effector memory T cells (mean of 68% and 69% in patients treated during acute/early and chronic infection, respectively).

T-Cell Receptors Found in Myeloid Cell Lysates. Myeloid cells have been proposed as a possible HIV-1 reservoir in patients on suppressive therapy (35–37). We sorted myeloid cells from both peripheral blood and GALT from the eight patients in this study. We detected HIV-1 DNA in peripheral blood myeloid cell preparations from three of the eight patients (2, 5, 6) and in GALT myeloid cell preparations from four of the eight patients (5–8). From patients 2, 5, and 6, we analyzed 1,866,667–4,065,801 myeloid cells from peripheral blood and found an HIV-1 infection frequency of 0.0001–0.0003% (Table 2, columns 9 and 10). From GALT, we analyzed 3,467–12,110 myeloid cells (patients 5–8) and found an HIV-1 infection frequency of 0.008–0.03% (Table 4, columns 7 and 8). To investigate the possibility of T cells in our sorted myeloid cell populations, we performed T-cell receptor (TCR) sequencing of the myeloid cell lysates found to harbor HIV-1 DNA. We identified TCRs in all of the samples where HIV-1 had been detected, indicating the presence of T cells (Fig. S2). We thus cannot rule out the possibility that the HIV-1 DNA found in the myeloid cell lysates actually came from infected T cells that remained in the sorted myeloid cells.

HIV-1 Populations from Plasma Collected Before Initiation of cART and Cells Isolated After Several Years of Suppressive Therapy Are Phylogenetically Similar. We conducted phylogenetic analyses to evaluate the genetic relationships between the HIV-1 DNA sequences from infected cells from peripheral blood and GALT and HIV-1 from plasma isolated after 4–12 y of suppressive therapy to viral RNA isolated from plasma before initiation of therapy. ML trees were reconstructed for *gag* and *pol* [p6 through nucleotides 1–900 of reverse transcriptase (RT)] sequences from the different T-cell populations and pretherapy plasma RNA. Before the tree construction each alignment was analyzed for the presence of G-to-A hypermutated sequences. G-to-A hypermutated sequences have been subjected to hypermutation by the cellular antiviral protein APOBEC3G and are believed to occur during one single replication cycle rather than through gradual sequence evolution. Approximately 30% of all of the sequences from cells isolated on-therapy were shown to be hypermutated and were therefore excluded from further analysis. Sequences from all eight patient samples as well as standard laboratory viruses formed independent populations that were at least 5% different from one another on a phylogenetic tree, with no intermingling, demonstrating that the viral populations in these patients were genetically distinct. For all patients analyzed, the phylogenetic distribution of intracellular DNA sequences from $CD4^+$ T cells in peripheral blood and GALT isolated after 4–12 y of suppressive therapy were similar to single-genome sequences derived from plasma virus RNA isolated before the initiation of antiretroviral therapy (subset of patients shown in Fig. 1). The intrapatient comparisons showed that all five patients who initiated therapy during acute/early infection had nearly monomorphic viral populations in both pretherapy plasma and cells isolated after 4–12 y of suppressive therapy (Fig. 1 *A* and *B* exemplifies this point). The homogeneity of viral sequences in patients treated during early infection contrasted with the higher level of diversity for sequences found in patients treated during chronic infection (examples shown in Fig. 1 *C* and *D*). In addition, we found that the HIV-1 RNA isolated from plasma collected during suppressive therapy was phylogenetically similar to pretherapy plasma RNA as well as on-therapy intracellular DNA.

To further analyze the genetic relationships between the sequences isolated from plasma before initiation of therapy (pretherapy) and the sequences isolated from cells in peripheral blood and GALT after 4–12 y of suppressive cART (on-therapy) in more detail, we conducted compartmentalization tests [tree based, association index (AI) and distances based, Wright's measure of population subdivision (F_{ST})] to assess whether the HIV-1 populations are structured by the different time points when they were isolated (before initiation or after several years of therapy) (Table 5). Hence, in this study, we have used compartmentalization tests to describe the genetic distance between two groups of sequences isolated at different time points rather than focusing on different tissue compartments. For sequences from patients where recombination was identified using a genetic algorithm for recombination detection (GARD), additional compartmentalization tests were performed for each nonrecombinant fragment (Table S2). Apart from the analysis comparing pre- and on-therapy sequences, we also conducted the same analyses comparing pretherapy plasma samples obtained at two different times from patients 6 and 8. The results from these analyses, when the patients were not receiving cART, help us to better evaluate the results we find in the patients during suppressive antiretroviral therapy.

We started by conducting a phylogenetic association analysis, which gives an estimate of the degree of viral compartmentalization. An AI value of 1 implies that the clustering of HIV-1 sequences does not deviate from that expected from random compartment association, whereas an AI value closer to 0 implies a strict genetic structuring by compartment. In the AI analysis, only bootstrap values above 0.95 were considered as significant evidence for compartmentalization. In the pretherapy plasma samples from patients 6 and 8, the AI was 0.03 and 0.26, respectively (Table 5, column 5). In contrast, the AI ranged from 0.61 to 1.00 in the patients treated during acute/early infection and from 0.50 to 0.79 in the patients treated during chronic infection. The high AI values between pre- and on-therapy sequences suggest random or nearly random clustering between HIV-1 RNA sequences from plasma isolated before initiation of therapy and HIV-1 DNA sequences from cells isolated from peripheral blood and GALT after several years of suppressive cART, indicating no genetic change during the years of therapy. We then conducted compartmentalization analysis using F_{ST}, which compares the

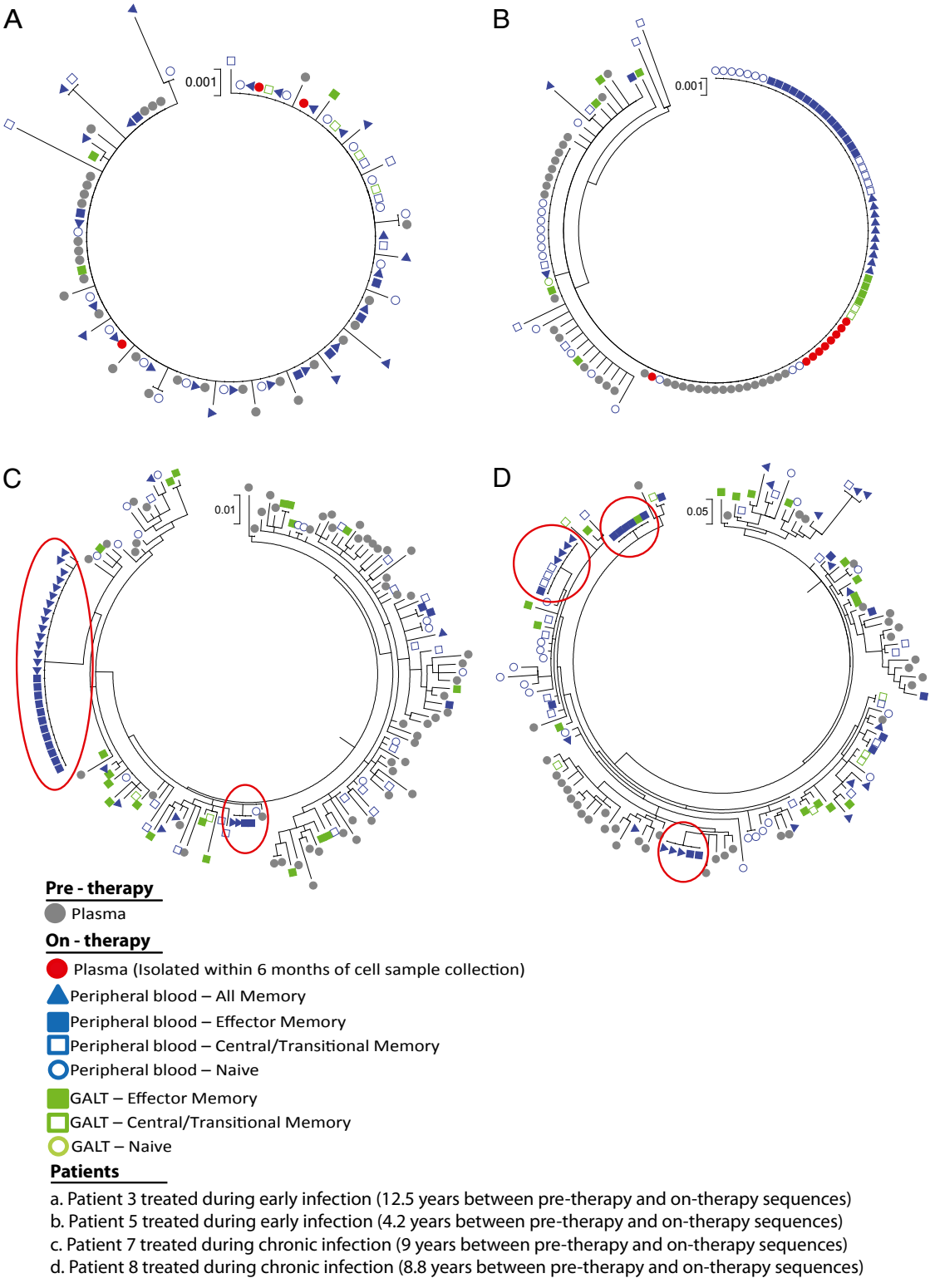

Fig. 1. Phylogenetic analysis of viral sequences from plasma isolated before the initiation of cART and cells isolated from peripheral blood and GALT after several years of suppressive cART. ML trees of sequences from pretherapy plasma (gray filled circles), on-therapy plasma (red filled circles), peripheral blood [all memory (blue filled triangles), central/transitional memory (blue filled squares), effector memory (blue open squares), and naïve (blue open circles) T cells], and GALT [central/transitional memory (green filled squares), effector memory (green open squares), and naïve (green open circles) T cells] from a subset of patients initiating antiviral therapy during acute/early HIV-1 infection (patients 3 and 5) (*A* and *B*), and during chronic HIV-1 infection (patients 7 and 8) (*C* and *D*: red circles indicate identical sequences isolated from different cells). Patient 7 initiated therapy in chronic infection and had identical clonal HIV-1 sequences containing a large 380-bp deletion (*C*). The trees representing the sequences isolated from patients 1, 2, 4, and 6 are in Fig. S3.

Table 5. Genetic compartmentalization, divergence, and evolutionary rate results

1	2	3	4	5	6	7	8	9	10	11
				Compartmentalization analysis*						
				Tree based		Genetic distance based		Evolutionary rate; nucleotide substitutions per site per y		
Patient	Sample	Years between samples	Time before pretherapy and initiation of therapy, d	AI[a]	Bootstrap significance	F_{ST}	Regression analysis, R^2	Mean	Lower 95% BCI	Upper 95% BCI
			Initiated therapy during chronic infection							
6	PT vs. PT	1.5	N/A	0.03	1	<0.001	0.78	7.10E-03	5.46E-03	8.86E-03
8	PT vs. PT	1.5	N/A	0.26	1	<0.001	0.17	5.01E-03	3.64E-03	6.44E-03
			Initiated therapy during early infection							
1	PT vs. OT	8.5	0	0.97	0.40	0.17	0.00	1.39E-04	4.61E-05	2.45E-04
2	PT vs. OT	7.6	0	0.61	0.95	0.01	0.11	2.97E-05	1.28E-06	7.26E-05
3	PT vs. OT	12.5	−14	1.00	0.31	0.59	0.00	8.70E-06	1.16E-06	2.14E-05
4	PT vs. OT	6.6	1	0.84	0.65	0.10	0.00	1.75E-05	1.21E-06	4.45E-05
5	PT vs. OT	4.3	12	0.86	0.59	0.14	0.00	3.50E-05	1.15E-06	9.22E-05
			Initiated therapy during chronic infection							
6[b]	PT vs. OT	5.3	40	0.58	1.00	<0.001	0.04	2.46E-05	1.13E-06	7.31E-05
7	PT vs. OT	9.8	180	0.79	0.91	<0.001	0.02	1.07E-04	5.74E-05	1.61E-04
8	PT vs. OT	8.8	0	0.50	1.00	<0.001	0.06	1.40E-04	3.86E-05	2.54E-04

BCI, Bayesian credible interval; OT, on-therapy; PT, pretherapy.

*P values <0.05 and bootstrap values >0.95 were considered statistically significant evidence of compartmentalization.

[a]AI, where 0 indicates maximum phylogenetic structure and 1 indicates panmixia. The two compartmentalization analyses were conducted with all sequences and with equal number of sequences in each group. The different ways to analyze the data did not lead to substantially different results.

[b]Results for this patient changed to no significant evidence of compartmentalization when running the same analyses with collapsed identical sequences.

mean pairwise genetic distance between two sequences from different compartments (pretherapy and on-therapy) to the mean distance between sequences from the same compartment. As shown in column 7 of Table 5, the F_{ST} analysis showed statistically significant support for a genetic subdivision of sequences isolated before initiation and after several years of therapy in patients 2 and 6–8 ($P \leq 0.01$) indicating a higher degree of structure than expected by chance for these patients. In addition, we detected evidence for compartmentalization in the nonrecombinant fragments for patient 1 ($P = 0.02$ and $P = 0.04$ for fragments 1 and 2, respectively), confirming that recombination can affect the power to detect compartmentalization (38). However, the corresponding AI values indicate that the extent of compartmentalization in all of these patients is low (Table S2, column 5).

Evidence Against Substantial HIV-1 Genetic Evolution During Suppressive Therapy. The genetic similarity between HIV-1 populations in plasma before the initiation of cART and HIV-1 populations in infected cells isolated after 4–12 y of suppressive antiretroviral therapy implies that little change accumulated at the nucleotide level during therapy. To further evaluate the degree of viral evolution during suppressive cART in these eight patients, we investigated the correlation of genetic divergence and time between the two time points (from before initiation of antiretroviral therapy to after 4–12 y of suppressive therapy, as well as between the two pretherapy plasma samples from patients 6 and 8) using linear regression analysis (root-to-tip analysis as implemented in Path-O-Gen, Institute of Evolutionary Biology, Ashworth Laboratories; http://tree.bio.ed.ac.uk/). This analysis estimates the correlation between genetic divergence and time, based on the estimated phylogenetic tree. A large correlation between genetic divergence and time would indicate that viral evolution has occurred between the viral sequences isolated before the initiation of therapy and the viral sequences isolated after several years of suppressive therapy, supporting a model in which there are productive cycles of viral replication during treatment. For the two pretherapy samples from patients 6 and 8, the estimated R^2 was 0.8 and 0.2, respectively. Notably, in one of the nonrecombinant fragments for patient 8, the R^2 was 0.54 (Table S2). In contrast, for the samples from patients treated during early infection, the estimated R^2 between genetic divergence and time ranged from 0.0006 to 0.1. Similar results were obtained for the samples from patients treated during chronic infection ($R^2 = 0.02$–0.06) (Table 5, column 8).

As a final analysis of the dynamics of HIV-1 during suppressive antiretroviral therapy, we estimated the evolutionary rate (nucleotide substitutions per site per year) for the RNA sequences isolated from plasma before initiation of cART and the DNA sequences from cells sorted from peripheral blood and GALT after 4–12 y of suppressive therapy using Bayesian evolutionary inference [implemented in Bayesian evolutionary analysis sampling trees (BEAST)] (39). We also estimated the evolutionary rate for the two pretherapy plasma samples from patients 6 and 8. As shown in column 9 of Table 5, we found a mean evolutionary rate of 7×10^{-3} and 5×10^{-3} nucleotide substitutions per site per year before these patients started therapy. These evolutionary rates in the two pretherapy samples are in agreement with other observations of HIV-1 evolutionary rates in absence of treatment (40). For the patients treated during acute/early infection, the evolutionary rate between the pre- and on-therapy sequences ranged from 9×10^{-6} to 1×10^{-4} nucleotide substitutions per site per year, which equates to a mean of 0.0097–0.15 changes in the sequence region analyzed per year during suppressive cART (based on the 1,110-bp long *gag–pol* region that we sequenced). For the patients treated during chronic infection, the evolutionary rate was estimated to range from 2×10^{-5} to 1×10^{-4} nucleotide substitutions per site per year. This equates to a mean of 0.03–0.1 changes in the viral region analyzed per year during suppressive cART in the patients treated during chronic infection. Hence the viral evolution in the T cells analyzed from these eight patients was extremely low during the years of suppressive antiretroviral therapy.

Evidence for Clonal T-Cell Proliferation as a Cause of Persistence. Interestingly, in samples from patient 7, who initiated therapy during chronic infection, we found identical clonal HIV-1 sequences

in effector and all memory T cells isolated from peripheral blood. This clonal sequence contained a large 380-bp deletion (base pairs 2,177–2,236 in HXB2 genome) essentially eliminating the protease from this HIV-1 population, indicating that this viral population was not replication competent and must be the result of the expansion of cells containing this replication-incompetent HIV-1 population. In addition to patient 7, we also found several cells harboring identical sequences in the two other patients treated during chronic infection (Fig. 1 *C* and *D*, red circles).

Discussion

The mechanisms that account for HIV-1 persistence during cART remain incompletely understood. We therefore performed a detailed analysis of HIV-1 DNA in various cell populations (naïve, memory, and myeloid cells) in blood and GALT from individuals who started therapy during either acute/early or chronic infection. Consistent with earlier reports, we found that the majority of HIV-1 DNA in both tissues (peripheral blood and GALT) and both patient groups (acute/early and chronic) was detected in the memory $CD4^+$ T-cell population and that the central/transitional memory population was the major contributor to the T-cell viral reservoir in peripheral blood (8, 9, 14). In contrast, we found that the effector memory population was the major contributor to the HIV-1 reservoir in GALT. In addition to HIV-1 infection in memory T cells, we also detected HIV-1 in isolated naïve T cells from both peripheral blood and GALT, although at much lower frequencies. Despite the low infection frequency and the small percentage that this cellular subset contributes to the total viral reservoir, the long life span of naïve T cells suggest they may still be an important viral reservoir in patients on long-term suppressive cART (15, 41). We found evidence that the HIV-1 infection frequencies of cells from peripheral blood were generally higher in patients who initiated therapy during chronic infection compared with patients who initiated therapy during acute/early infection, as has been observed by others (14, 42), and extended these findings to confirm similar trends in GALT.

There were significant differences in the nature of the reservoir in blood and GALT. For example, although we found that the HIV-1 viral burden in the memory T-cell populations from GALT was similar to that in peripheral blood, the overall HIV-1 burden was more concentrated in central/transitional memory T cells in peripheral blood and effector memory T cells in GALT. The fact that we find effector memory T cells being the larger viral reservoir in GALT is consistent with higher frequency of infection and higher percentage of effector memory cells located in this anatomical site. However, due to limited availability of cells from GALT, our analyses were restricted to very few cells, and further confirmation of these findings is therefore required. When all cell types were combined, we did not find a statistically significant difference in infection frequency between GALT and blood (although the confidence interval included more than threefold differences in either direction). This result is in disagreement with earlier observations (17) but consistent with a study by Chomont et al. (14).

In addition to T cells, monocytes/macrophages are believed to become infected in persons with HIV-1. The role these cells play in patients on suppressive cART is not fully understood (43–45). We sorted myeloid cells from both peripheral blood and GALT from all of the eight patients and found HIV-1 DNA in myeloid cells from peripheral blood and GALT in three and four of the eight patient samples, respectively. In all of the myeloid samples where we found HIV-1 DNA, we also found the presence of TCRs. The purity of the myeloid sort from peripheral blood was 83–97%, and, therefore, we cannot rule out that the HIV-1 DNA we found in the myeloid cell lysates came from the presence of T cells. However, our results do indicate that if myeloid cells from peripheral blood and GALT are infected, the frequency is extremely low.

Latently infected T cells are clearly a key HIV-1 reservoir in patients on long-term suppressive cART. The dynamics of this reservoir and whether it is replenished by residual HIV-1 replication during suppressive cART is not fully understood. We compared the intracellular and plasma-derived viral sequences from the eight patients after several years of therapy to single-genome sequences from plasma collected before the initiation of cART to assess whether there was evidence of genetic evolution, which would support that residual viral replication contributes to the maintenance of the HIV-1 reservoir. The phylogenetic distribution of intracellular HIV-1 DNA and plasma-derived HIV-1 RNA sequences from patients after years of therapy were similar to single-genome sequences derived from plasma virus RNA isolated before the initiation of antiretroviral therapy. The similarity of the sequences isolated before initiation of therapy to the sequences isolated after several years on suppressive cART was more apparent in the patients treated during acute/early infection when the HIV-1 populations are genetically homogeneous. In samples from the three patients treated during chronic infection, the viral populations were more diverse and few sequences were identical. However, ML trees revealed that pretherapy RNA sequences and intracellular DNA sequences from cells collected after years of suppressive cART were phylogenetically similar.

When conducting compartmentalization analysis, no clear sign of structure between the pre- and on-therapy sequences was detected in the patients treated during acute/early infection except for patient 2, where we found evidence for compartmentalization in both the AI and F_{ST} analyses. In the patients treated during chronic infection, we found evidence for compartmentalization in both of the analyses. However, the corresponding AI values indicate that the compartmentalization is low between the pre- and on-therapy sequences in these patients. These observations suggest that there are few differences between the sequences found in plasma isolated before the initiation of therapy and the sequences in cells isolated after long-term suppressive therapy, indicating that the HIV-1 reservoir during suppressive therapy is stable and not maintained by on-going replication.

To further evaluate whether on-going viral replication takes place during long-term suppressive HIV-1 therapy, we conducted two additional analyses (correlation of genetic divergence and time, and estimation of rate of evolution) to quantify the amount of viral change and evolution during suppressive cART. In all of the eight patients we found limited correlation of genetic divergence and time between the HIV-1 sequences from the pretherapy plasma samples and on-therapy cell samples, suggesting lack of substantial on-going evolution during suppressive cART. When estimating the evolutionary rate of the HIV-1 sequences between the pretherapy and on-therapy time points, we found a very low evolutionary rate between these two time points in the patients treated during both early and chronic infection. The evolutionary rates obtained from our analysis are however likely to be even lower because there was insufficient information in the sequence data to make posterior estimates diverge from the prior expectation in the Bayesian analysis. An informative but diffuse prior specification was required to be able to perform the analyses in the absence of signal for divergence accumulation.

The small sample size limits some of our ability to generalize results and there may be some patient populations or treatment contexts that would produce different results. However, based on the compartmentalization, regression, and evolutionary rate analyses, we arrive at several conclusions. First, there was evidence for genetic compartmentalization between pre- and on-therapy sequences in four (2, 6–8) of the eight patients. The AI, however, showed that the degree of compartmentalization was low. Second, no clear correlation between divergence and time was detected in any of the patient samples. Third, evolutionary rate estimates indicate an extremely low nucleotide change during the years of suppressive therapy. An important limitation in our study is that the pretherapy samples for some of the patients were collected 12–180 d before the initiation of therapy. Thus, the viral change detected in the patients could be due, at least in part, to accumulation of nucleotide substitutions during the days when the patients were not on therapy. Another limitation is that we cannot exclude the occurrence of small bursts of viral

replication, which leave little genetic trace to be identified using phylogenetic analyses. Nevertheless, our findings suggest that if such viral bursts of replication occur, they make a limited contribution to the latent HIV-1 reservoir in the patient samples analyzed in this study. In addition, our methods do not distinguish whether the HIV-1 DNA under analysis is integrated, linear, or circular. As these patients have been on suppressive cART for many years, most of the HIV-1 DNA can be assumed to be in an integrated form (34), however, we do not know if the sequences under analysis will produce a replication-competent virus. Moreover, Eriksson et al. have recently showed that there is little correlation between the number of HIV-1–infected cells and the amount of replication-competent virus during long-term suppressive HIV-1 therapy (46).

The role of homeostatic proliferation of memory T-cell populations as a cause of persistence has not been well defined in humans. Previous studies have suggested that cellular proliferation of transitional memory T cells and naïve T cells also maintain the HIV-1 reservoir in patients on suppressive cART, but the evidence was indirect (14, 15). We identified a single individual treated during chronic infection whose virus population was enriched for a single clone containing a 380-bp deletion, which essentially eliminated the protease gene. Assuming a single infection event resulted in the seeding of this virus population, the only manner by which this population would dominate would be through clonal proliferation and expansion of this infected T cell. However, due to the fact that this viral variant is defective, we cannot determine if homeostatic proliferation maintains replication-competent HIV-1. It is, however, tempting to speculate that the predominant plasma clones identified by Bailey et al. (27) arise from proliferating cells with replication-competent HIV-1.

In conclusion, our results from peripheral blood and GALT samples isolated from these eight patients on long-term suppressive therapy indicate that early initiation of effective therapy results in lower reservoir size in blood and GALT than later initiation of therapy. This suggests that persons who initiate therapy very early in infection may be an important group in which to test future efforts aimed at eliminating viral reservoirs. The evidence against substantial HIV-1 genetic evolution in the HIV-1–infected $CD4^+$ T-cell populations after up to 12 y of therapy suggests that virus replication is not the major cause of viral persistence in these cell populations. The presence of clonal intracellular HIV-1 sequences indicates that HIV-1–infected memory T cells homeostatically proliferate during suppressive therapy, but whether this cellular mechanism contributes to the numbers of replication-competent HIV-1 strains is unknown.

Materials and Methods

Clinical Specimens. Paired GALT and peripheral blood samples from eight HIV-1 subtype B individuals were analyzed. The samples were obtained from individuals in the Options Cohort at the University of California, San Francisco (UCSF). The Options Cohort is an ongoing longitudinal observational cohort study of adults enrolled within 6 mo of HIV-1 antibody seroconversion and followed throughout the course of HIV-1 disease. In this study, we included five patients who had elected to begin therapy within 30 d of entering the cohort (acute/early infection, patients 1–5) and three who had chosen to begin therapy more than 1 y after infection (chronic infection, patients 6–8) (Table 1). The criterion we used for selection of these patients was undetectable viremia (<40–75 copies per mL) for at least 3 y after the initiation of therapy. Informed consent was obtained from all eight patients. The study was approved by the institutional review boards at UCSF and the Karolinska Institutet.

Single-Proviral Sequencing. To quantify and genetically characterize HIV-1 viral populations in the cells isolated from peripheral blood and GALT, we used the single-proviral sequencing assay (47). This assay has been described before, but briefly, sorted cells are lysed and serially diluted and single HIV-1 molecules are PCR amplified using primers flanking the p6–RT region. To obtain PCR products derived from single HIV-1 DNA molecules, the cellular lysate with HIV-1 DNA was serially diluted 1:3 to a maximum dilution of 1:243. PCR amplification (p6 through nucleotides 1–900 of RT) and sequencing of the DNA in each well allowed enumeration and analysis of the genetic relationship of viral DNA molecules in infected cell type. The single-proviral sequencing assay was used as previously described with minor changes described in *SI Materials and Methods, Single-Proviral Sequencing*.

Single-Genome Sequencing. To compare the intracellular populations identified using the single-proviral sequencing assay to HIV-1 RNA populations found in plasma collected before initiation of antiretroviral therapy, we performed single-genome sequencing (SGS) on the plasma samples from each of the eight patients as described earlier (48–50). To extract viral RNA from plasma collected during suppressive therapy, we used a modified version of the SGS method. This involved ultracentrifugation of at least 28 mL of plasma per patient to pellet the virus. From patients 1–3, 5, and 6 we were able to extract viral RNA from additional large plasma volume samples collected 6 mo after the cells were sorted. The viral region amplified from plasma span from p6 through RT and was the same region that was amplified from intracellular viral DNA.

Statistical Methods. We estimated the HIV-1 infection frequency in each cell type using an ML statistical analysis as described in *SI Materials and Methods, Statistical Methods*, building on methods described previously (47).

Phylogenetic Analyses. Contigs of the intracellular and extracellular HIV-1 populations were generated from the raw sequencing data using an in-house computer program written in Perl scripting language (available upon request). Recombination was screened using a GARD (51) and all analyses were subsequently performed in separate for each nonrecombinant fragment (Table S2). For phylogenetic analysis of the HIV-1 populations, ML phylogenetic trees were constructed in phylogenetic estimation using maximum likelihood version 3.0 (52) using SeaView version 4.0 platform (53). We used the general time-reversible (GTR) nucleotide substitution model incorporating gamma-distributed rate variation among sites and allowing a proportion of invariable sites. Our heuristic tree search strategy used the subtree pruning and regrafting and the nearest neighbor interchanges branch-swapping algorithms. Branch support was inferred using 1,000 bootstrap replicates. Evolutionary divergence was explored using root-to-tip analysis as implemented in Path-O-Gen.

Evidence for compartmentalization between pretherapy sequences from plasma and on-therapy sequences from peripheral blood and GALT was first scrutinized using the tree-based method Simmond's AI (54). AI statistical support was obtained using 1,000 bootstrap trees and 10 random relabelings per sample (only bootstrap values above 0.95 were considered significant). In addition, we used nucleotide distance-based methods that do rely on phylogenies, which are often poorly resolved for intrahost evolution (38). Particularly, we estimated F_{ST} (55). Distances were estimated using an ML approach under a GTR nucleotide substitution model, estimating all parameters independently for each branch. To obtain the significance of the statistics, 10,000 permutations were computed, with the permutation test randomly allocating sequences into GALT or peripheral blood predefined clades. The two compartmentalization tests were performed using the hypothesis testing using phylogenies package (56). To estimate the rate of evolutionary change, we conducted a Bayesian Markov chain Monte Carlo (MCMC) analysis implemented in BEAST (39). We used the same nucleotide substitution model settings as in the ML analysis described above. A strict molecular clock was used with a flexible Bayesian skyride tree prior (57). To ensure convergence in case data sets did not contain sufficient temporal signal, we performed all analyses using a log-normal prior distribution with a mean of −10 and a SD of 1.5 on the evolutionary rate, which is still sufficiently diffuse to allow for higher rates in case temporal signal would be present. Each nonrecombinant fragment was allowed to have different phylogenetic trees, while sharing the same substitution and clock model. MCMC analysis was run typically for 50–150 million steps, discarding a 10% burn-in, and convergence of the chains was inspected using Tracer, Institute of Evolutionary Biology, Ashworth Laboratories (http://tree.bio.ed.ac.uk/).

ACKNOWLEDGMENTS. We thank the patients participating in this study. This work was primarily supported by an amfAR Research Consortium on HIV Eradication (ARCHE) Collaborative Research Grant from The Foundation for AIDS Research (amfAR 107857-48-RGRL) and Delaney AIDS Research Enterprise (U19 AI096109). The work was also supported by the Swedish International Development Agency (SWE-2009-046), The Swedish Research Council (K2011-56X-21749-01-6), the National Institutes of Health (NIH) [(AI071713, K24AI069994, and K23 CA157929), the UCSF–Gladstone Institute of Virology and Immunology Center for AIDS Research (P30AI027763 and P30 MH59037), the NIH/National Center for Research Resources UCSF–Clinical and Translational Science Institute (UL1RR024131), the European Union Seventh Framework Programme [FP7/2007-2013] under Grant Agreement 278433-PREDEMICS, and European Research Council Grant Agreement

260864. L.J. was supported by the Erik and Edith Fernström Foundation for Medical Research and by Karolinska Institutet alumni funds. N.R.F. is supported by Fundação para a Ciência e Tecnologia under Grant Agreement SFRH/BD/64530/2009.

1. Deeks SG, et al.; International AIDS Society Scientific Working Group on HIV Cure (2012) Towards an HIV cure: A global scientific strategy. *Nat Rev Immunol* 12(8): 607–614.
2. Dornadula G, et al. (1999) Residual HIV-1 RNA in blood plasma of patients taking suppressive highly active antiretroviral therapy. *JAMA* 282(17):1627–1632.
3. Havlir DV, et al.; Gilead 903 Study Team (2005) Predictors of residual viremia in HIV-infected patients successfully treated with efavirenz and lamivudine plus either tenofovir or stavudine. *J Infect Dis* 191(7):1164–1168.
4. Maldarelli F, et al. (2007) ART suppresses plasma HIV-1 RNA to a stable set point predicted by pretherapy viremia. *PLoS Pathog* 3(4):e46.
5. Zhang L, et al. (1999) Quantifying residual HIV-1 replication in patients receiving combination antiretroviral therapy. *N Engl J Med* 340(21):1605–1613.
6. Lewin SR, et al. (1999) Use of real-time PCR and molecular beacons to detect virus replication in human immunodeficiency virus type 1-infected individuals on prolonged effective antiretroviral therapy. *J Virol* 73(7):6099–6103.
7. Palmer S, et al. (2008) Low-level viremia persists for at least 7 years in patients on suppressive antiretroviral therapy. *Proc Natl Acad Sci USA* 105(10):3879–3884.
8. Chun TW, et al. (1998) Early establishment of a pool of latently infected, resting CD4 (+) T cells during primary HIV-1 infection. *Proc Natl Acad Sci USA* 95(15):8869–8873.
9. Finzi D, et al. (1997) Identification of a reservoir for HIV-1 in patients on highly active antiretroviral therapy. *Science* 278(5341):1295–1300.
10. Wong JK, et al. (1997) Recovery of replication-competent HIV despite prolonged suppression of plasma viremia. *Science* 278(5341):1291–1295.
11. Burke B, et al. (2007) Primary cell model for activation-inducible human immunodeficiency virus. *J Virol* 81(14):7424–7434.
12. Saleh S, et al. (2007) CCR7 ligands CCL19 and CCL21 increase permissiveness of resting memory CD4+ T cells to HIV-1 infection: A novel model of HIV-1 latency. *Blood* 110(13):4161–4164.
13. Swiggard WJ, et al. (2005) Human immunodeficiency virus type 1 can establish latent infection in resting CD4+ T cells in the absence of activating stimuli. *J Virol* 79(22): 14179–14188.
14. Chomont N, et al. (2009) HIV reservoir size and persistence are driven by T cell survival and homeostatic proliferation. *Nat Med* 15(8):893–900.
15. Wightman F, et al. (2010) Both CD31(+) and CD31$^-$ naive CD4(+) T cells are persistent HIV type 1-infected reservoirs in individuals receiving antiretroviral therapy. *J Infect Dis* 202(11):1738–1748.
16. Palmer S, Josefsson L, Coffin JM (2011) HIV reservoirs and the possibility of a cure for HIV infection. *J Intern Med* 270(6):550–560.
17. Chun TW, et al. (2008) Persistence of HIV in gut-associated lymphoid tissue despite long-term antiretroviral therapy. *J Infect Dis* 197(5):714–720.
18. Yukl SA, et al. (2010) Differences in HIV burden and immune activation within the gut of HIV-positive patients receiving suppressive antiretroviral therapy. *J Infect Dis* 202(10):1553–1561.
19. Anton PA, et al. (2003) Multiple measures of HIV burden in blood and tissue are correlated with each other but not with clinical parameters in aviremic subjects. *AIDS* 17(1):53–63.
20. Di Stefano M, et al. (2001) Intracellular and cell-free (infectious) HIV-1 in rectal mucosa. *J Med Virol* 65(4):637–643.
21. Lampinen TM, et al. (2000) Association of antiretroviral therapy with detection of HIV-1 RNA and DNA in the anorectal mucosa of homosexual men. *AIDS* 14(5):F69–F75.
22. Poles MA, et al. (2006) Lack of decay of HIV-1 in gut-associated lymphoid tissue reservoirs in maximally suppressed individuals. *J Acquir Immune Defic Syndr* 43(1):65–68.
23. Evering TH, et al. (2012) Absence of HIV-1 evolution in the gut-associated lymphoid tissue from patients on combination antiviral therapy initiated during primary infection. *PLoS Pathog* 8(2):e1002506.
24. Kieffer TL, et al. (2004) Genotypic analysis of HIV-1 drug resistance at the limit of detection: Virus production without evolution in treated adults with undetectable HIV loads. *J Infect Dis* 189(8):1452–1465.
25. Mens H, et al. (2007) Investigating signs of recent evolution in the pool of proviral HIV type 1 DNA during years of successful HAART. *AIDS Res Hum Retroviruses* 23(1): 107–115.
26. Persaud D, et al. (2007) Slow human immunodeficiency virus type 1 evolution in viral reservoirs in infants treated with effective antiretroviral therapy. *AIDS Res Hum Retroviruses* 23(3):381–390.
27. Bailey JR, et al. (2006) Residual human immunodeficiency virus type 1 viremia in some patients on antiretroviral therapy is dominated by a small number of invariant clones rarely found in circulating CD4+ T cells. *J Virol* 80(13):6441–6457.
28. Nottet HS, et al. (2009) HIV-1 can persist in aged memory CD4+ T lymphocytes with minimal signs of evolution after 8.3 years of effective highly active antiretroviral therapy. *J Acquir Immune Defic Syndr* 50(4):345–353.
29. Kim H, Perelson AS (2006) Viral and latent reservoir persistence in HIV-1-infected patients on therapy. *PLOS Comput Biol* 2(10):e135.
30. Dinoso JB, et al. (2009) Treatment intensification does not reduce residual HIV-1 viremia in patients on highly active antiretroviral therapy. *Proc Natl Acad Sci USA* 106(23):9403–9408.
31. McMahon D, et al. (2010) Short-course raltegravir intensification does not reduce persistent low-level viremia in patients with HIV-1 suppression during receipt of combination antiretroviral therapy. *Clin Infect Dis* 50(6):912–919.
32. Buzón MJ, et al. (2010) HIV-1 replication and immune dynamics are affected by raltegravir intensification of HAART-suppressed subjects. *Nat Med* 16(4):460–465.
33. Yukl SA, et al. (2010) Effect of raltegravir-containing intensification on HIV burden and T-cell activation in multiple gut sites of HIV-positive adults on suppressive antiretroviral therapy. *AIDS* 24(16):2451–2460.
34. Mexas AM, et al. (2012) Concurrent measures of total and integrated HIV DNA monitor reservoirs and ongoing replication in eradication trials. *AIDS* 26(18):2295–2306.
35. Zhu T, et al. (2002) Evidence for human immunodeficiency virus type 1 replication in vivo in CD14(+) monocytes and its potential role as a source of virus in patients on highly active antiretroviral therapy. *J Virol* 76(2):707–716.
36. Lambotte O, et al. (2000) Detection of infectious HIV in circulating monocytes from patients on prolonged highly active antiretroviral therapy. *J Acquir Immune Defic Syndr* 23(2):114–119.
37. Zalar A, et al. (2010) Macrophage HIV-1 infection in duodenal tissue of patients on long term HAART. *Antiviral Res* 87(2):269–271.
38. Zárate S, Pond SL, Shapshak P, Frost SD (2007) Comparative study of methods for detecting sequence compartmentalization in human immunodeficiency virus type 1. *J Virol* 81(12):6643–6651.
39. Drummond AJ, Suchard MA, Xie D, Rambaut A (2012) Bayesian phylogenetics with BEAUti and the BEAST 1.7. *Mol Biol Evol* 29(8):1969–1973.
40. Lemey P, Rambaut A, Pybus OG (2006) HIV evolutionary dynamics within and among hosts. *AIDS Rev* 8(3):125–140.
41. Michie CA, McLean A, Alcock C, Beverley PC (1992) Lifespan of human lymphocyte subsets defined by CD45 isoforms. *Nature* 360(6401):264–265.
42. Strain MC, et al. (2005) Effect of treatment, during primary infection, on establishment and clearance of cellular reservoirs of HIV-1. *J Infect Dis* 191(9):1410–1418.
43. Almodóvar S, et al. (2007) HIV-1 infection of monocytes is directly related to the success of HAART. *Virology* 369(1):35–46.
44. Ellery PJ, et al. (2007) The CD16+ monocyte subset is more permissive to infection and preferentially harbors HIV-1 in vivo. *J Immunol* 178(10):6581–6589.
45. Fulcher JA, et al. (2004) Compartmentalization of human immunodeficiency virus type 1 between blood monocytes and CD4+ T cells during infection. *J Virol* 78(15): 7883–7893.
46. Eriksson S, et al. (2013) Comparative analysis of measures of viral reservoirs in HIV-1 eradication studies. *PLoS Pathog* 9(2):e1003174.
47. Josefsson L, et al. (2012) Hematopoietic precursor cells isolated from patients on long-term suppressive HIV therapy did not contain HIV-1 DNA. *J Infect Dis* 206(1):28–34.
48. Palmer S, et al. (2005) Multiple, linked human immunodeficiency virus type 1 drug resistance mutations in treatment-experienced patients are missed by standard genotype analysis. *J Clin Microbiol* 43(1):406–413.
49. Kearney M, et al. (2009) Human immunodeficiency virus type 1 population genetics and adaptation in newly infected individuals. *J Virol* 83(6):2715–2727.
50. Kearney M, et al. (2008) Frequent polymorphism at drug resistance sites in HIV-1 protease and reverse transcriptase. *AIDS* 22(4):497–501.
51. Kosakovsky Pond SL, Posada D, Gravenor MB, Woelk CH, Frost SDW (2006) GARD: A genetic algorithm for recombination detection. *Bioinformatics* 22(24):3096–3098.
52. Guindon S, et al. (2010) New algorithms and methods to estimate maximum-likelihood phylogenies: Assessing the performance of PhyML 3.0. *Syst Biol* 59(3):307–321.
53. Gouy M, Guindon S, Gascuel O (2010) SeaView version 4: A multiplatform graphical user interface for sequence alignment and phylogenetic tree building. *Mol Biol Evol* 27(2):221–224.
54. Wang TH, Donaldson YK, Brettle RP, Bell JE, Simmonds P (2001) Identification of shared populations of human immunodeficiency virus type 1 infecting microglia and tissue macrophages outside the central nervous system. *J Virol* 75(23):11686–11699.
55. Hudson RR, Slatkin M, Maddison WP (1992) Estimation of levels of gene flow from DNA sequence data. *Genetics* 132(2):583–589.
56. Pond SL, Frost SD, Muse SV (2005) HyPhy: Hypothesis testing using phylogenies. *Bioinformatics* 21(5):676–679.
57. Minin VN, Bloomquist EW, Suchard MA (2008) Smooth skyride through a rough skyline: Bayesian coalescent-based inference of population dynamics. *Mol Biol Evol* 25(7):1459–1471.